ESC European Society of Cardiology

Cardiovascular Research (2017) **113**, 1776–1788
doi:10.1093/cvr/cvx175

Cgnl1, an endothelial junction complex protein, regulates GTPase mediated angiogenesis

Ihsan Chrifi[1†], Dorien Hermkens[1†], Maarten M. Brandt[1], Christian G. M. van Dijk[2], Petra E. Bürgisser[1], Remco Haasdijk[1], Jiayi Pei[2], Esther H. M. van de Kamp[1], Changbin Zhu[3], Lau Blonden[1], Johan M. Kros[3], Dirk J. Duncker[2], Henricus J. Duckers[4†], and Caroline Cheng[1,2*†]

[1]Department of Cardiology, Thoraxcenter, Erasmus University Medical Center, Rotterdam, PO Box 2040, 3000 CA Rotterdam, The Netherlands; [2]Department of Nephrology and Hypertension, University Medical Center Utrecht, Utrecht, The Netherlands; [3]Department of Pathology, Erasmus University Medical Center Rotterdam, Rotterdam, The Netherlands; and [4]Department of Interventional Cardiology, University Medical Center Utrecht, Utrecht, The Netherlands

Received 25 November 2016; revised 19 June 2017; editorial decision 11 July 2017; accepted 29 August 2017; online publish-ahead-of-print 31 August 2017

Time for primary review: 38 days

Aims The formation of cell–cell and cell–extra cellular matrix (ECM) contacts by endothelial cells (ECs) is crucial for the stability and integrity of a vascular network. We previously identified cingulin-like 1 (Cgnl1) in a transcriptomic screen for new angiogenic modulators. Here we aim to study the function of the cell–cell junction associated protein Cgnl1 during vessel formation.

Methods and results Unlike family member cingulin, Cgnl1 expression is enriched in ECs during vascular growth. Cgnl1 is important for the formation of multicellular tubule structures, as shown *in vitro* using loss-of function assays in a 3D matrix co-culture system that uses primary human ECs and supporting mural cells. Further studies revealed that Cgnl1 regulates vascular growth by promoting Ve-cadherin association with the actin cytoskeleton, thereby stabilizing adherens junctions. Cgnl1 also regulates focal adhesion assembly in response to ECM contact, promoting vinculin and paxillin recruitment and focal adhesion kinase signalling. *In vivo*, we demonstrate in a postnatal retinal vascular development model in mice that Cgnl1 function is crucial for sustaining neovascular growth and stability.

Conclusions Our data demonstrate a functional relevance for Cgnl1 as a defining factor in new vessel formation both *in vitro* and *in vivo*.

Keywords Angiogenesis • Cgnl1 • Focal adhesion • Adherens junctions • Ve-cadherin

1. Introduction

New vessel formation plays a critical role in embryonic development and disease progression of adult organisms. The mechanism is complex and consists of multiple stages that include primary plexus formation, network expansion, and vascular remodelling.[1,2] During the initial phase of new vessel formation, maturing endothelial cells (ECs) establish cell–cell interaction to form multi-cellular structures that are gradually remodelled into microvascular tubules with open lumina. This critical step is orchestrated by mobilizing the EC's actin cytoskeleton to facilitate cell-morphological adaptations that are crucial for intercellular junction assembly. The importance of small GTPases in these processes has been previously investigated[3]: Rac1 is implied to be the predominant GTPase involved in VEGFA mediated angiogenesis,[4] and is crucial for lumen and tubule formation. Rac1 also facilitates migration as it controls actin polymerization during the formation of lamellopodia,[5] and knockdown of Rac1 in mice led to embryonic lethality as a result of defects in vascular growth.[6] In addition, cdc42 and Rac1 regulate endothelial barrier function by modulating the interaction between the actin cytoskeleton and junctional proteins like Ve-cadherin, located at adherence junctions.[7,8] Rho family GTPases constantly cycle between the guanine diphosphate bound inactive state and the guanine triphosphate (GTP) bound active

* Corresponding author. Tel: +31 10 7038066; fax: +31 10 7044769, E-mail: c.cheng@erasmusmc.nl

† The first two authors and the last two authors contributed equally to the study.

© The Author 2017. Published by Oxford University Press on behalf of the European Society of Cardiology.

This is an Open Access article distributed under the terms of the Creative Commons Attribution Non-Commercial License (http://creativecommons.org/licenses/by-nc/4.0/), which permits non-commercial re-use, distribution, and reproduction in any medium, provided the original work is properly cited. For commercial re-use, please contact journals.permissions@oup.com

state. Their activity is tightly regulated by their activators Guanine Exchange Factors (GEF), and their inhibitors, which include GTPase activation proteins and guanine-diphosphate-disassociation inhibitors.[9]

Cingulin is a 140 kDa protein, which is ubiquitously expressed in different cell types with high expression levels detected in epithelial cells of various origins. *In vitro* studies in canine renal epithelial cells demonstrates that cingulin is localized at the cytoplasmatic surface of tight junctions where it functions as an adaptor protein for GEFs.[10] Cingulin binds to actin filament bundles, suggesting that cingulin may be a linking protein between tight junction complexes and the actin cytoskeleton. However, although cingulin depletion promotes RhoA activity, it does not affect tight junction complex formation or actin cytoskeleton assembly.[10,11] Cingulin-like 1 (Cgnl1), a 150–160 kDa paralogue of cingulin, also known as JACOP and PCING, was recently discovered to be localized in both adherens and tight junctions. Cgnl1 was shown to be an inhibitor of RhoA activity, but was also involved in the activation of Rac1 by the GEF Tiam1 in epithelial cells.[10,12] Like cingulin, Cgnl1 is co-localized with actin filament bundles, implying that it could be a cross-road modulator that links intercellular junction assembly to actin cytoskeleton-regulated morphogenesis, both key processes in angiogenesis. Indeed, Cngl1 mRNA expression has been detected in CD31+ cells isolated from mouse embryos on days 8.5 and 9.5, in which it was preferentially expressed in endocardial cells, but not yolk sac ECs.[13] Previously, we conducted a genome-wide transcriptomic screen with the goal to identify new molecular regulators of vascular development during murine embryogenesis.[14] In line with the previous report, we found that unlike cingulin, Cgnl1 was mainly expressed in Flk1+ endothelial precursor cells during embryonic development. Cgnl1 has been indicated to be actively involved in tight junction regulation of ECs.[15] Here we further assessed the role of Cgnl1 in EC biology and angiogenesis.

Our data demonstrate that Cgnl1 promotes angiogenesis by strengthening adherens junctions via Rac1 activation, which leads to stabilization and further elongation of newly formed vascular tubules.

2. Methods

2.1 Mouse retinal angiogenesis model

Approval was granted by the institutional ethics review board (DEC 109-11-12). All animal procedures were conducted conform the guidelines from Directive 2010/63/EU of the European Parliament on the protection of animals used for scientific purposes. Two or 8-days old C57bl/6 pups were anesthetized by placement on ice. For Cgnl1 silencing experiments, 100 nmol accel siRNA targeting murine Cgnl1 was intravitreally injected in the left, and 100 nmol accel scrambled non-tageting siRNA in the right eye (Dharmacon, Netherlands) in a volume of 0.5 µl using a 33-gauge needle. At Day 6 or 12 post-transfection, pups were sacrificed by decapitation, and retinas were stained with FITC isolectin IB4 (1:200). Angiosys analysis software (Angiosystems, UK) was used to determine total tubule length, and the number of tubules and junctions per field of view. Adequate target mRNA inhibition was validated by qPCR analysis and western blot analysis.

2.2 *In vitro* culture

Human Umbilical Vein ECs (HUVECs; Lonza) and Human Brain Vascular Pericytes (HBVPs; Lonza) were cultured on gelatine-coated plates in EGM2 medium (EBM2 medium supplemented with EGM2 bullet kit and 2% FCS; Lonza) and DMEM (10% FCS; Lonza) respectively, in 5% CO_2 at 37°C. The experiments were performed with cells at Passage 3–5. Lentiviral transfected HUVECs that express green fluorescent protein (GFP) were used at Passage 6–8.

2.3 Statistical analysis

Results are expressed as the mean ± SD and statistical analysis was performed by one-way ANOVA followed by tukey's *post-hoc* test, or Student's *t*-test where appropriate. $P < 0.05$ was considered significant.

More detailed descriptions of the material and methods used in this study are provided in the Supplementary Material.

3. Results

3.1 Cgnl1 shows predominant expression in developing vascular structures

Cgnl1 was mainly expressed in the (fetal kinase receptor 1) Flk1+ cell population during embryonic development in mice as shown by qPCR validation of microarray screen data (*Figure 1A*). Cgnl1 was predominantly expressed in Flk1+ endothelial precursor cells at 9.5 days post-coitus during which the majority of the vascular structures in the embryo are established (*Figure 1A*). This finding was further confirmed by data-mining of public expression databases (NCBI, Gene Expression Omnibus: see Supplementary material online, *Figure S1A* and *B*), which showed higher expression levels of Cgnl1 in primary ECs of different origins compared with the more epithelial enriched expression of cingulin.

Next, whole mount *in situ* hybridization was conducted using a probe that targeted the zebrafish orthologue of Cgnl1 in the larval stages. At 24 h post-fertilization (hpf), Cgnl1 expression was observed in the trunk region in the dorsal aorta (DA) and post-cardinal vein with low expression in the intersegmental vessels (*Figure 1B* and *D*). In the head region, Cgnl1 was clearly expressed in the bi-lateral aorta Y-trunk and the cranial vasculature (*Figure 1E* and *C*). From 48 hpf onward, Cgnl1 expression was also observed in the heart (*Figure 1F*). The vascular expression pattern of Cgnl1 was similar to the vascular GFP pattern of Tg(kdrl; eGFP)^{y1} zebrafish larvae (see Supplementary material online, *Figure S1C*). This vascular pattern of Cngl1 gradually declined during larvae maturation (*Figure 1F–I*). Specific targeting of Cgnl1 by anti-sense probe was validated by comparing the anti-sense and sense probe signal (see Supplementary material online, *Figure S1D* and *E*). To assess if this vascular expression pattern was conserved in mammals, qPCR analysis was conducted on different organs in mature C57/bl6 mice. Endogenous murine Cgnl1 expression was significantly higher in the aorta and kidney as compared with heart, lung, liver, skeletal muscle, eye, and brain tissue (*Figure 1J*). In contrast, cingulin expression was not enriched in murine aorta (*Figure 1K*). HUVECs showed significant higher expression of Cgnl1 as compared with human pericytes, renal epithelial cells and fibroblasts (see Supplementary material online, *Figure S1F*). In contrast, cingulin expression was more prominent in renal epithelial cells (see Supplementary material online, *Figure S1G*). Immunohistological analysis demonstrated selective Cgnl1 expression in the endothelial lining of large blood vessels and microvessels in human samples (*Figure 1L*).

3.2 Cgnl1 is essential for neovascular tubule formation

Based on the vascular enriched expression profile of Cgnl1, we hypothesized that Cgnl1 contributes to vascular development. A standard 2D-matrigel sprouting assay was conducted in which sprouting capacity of ECs was assessed. In this assay, ECs form cordlike structures consisting

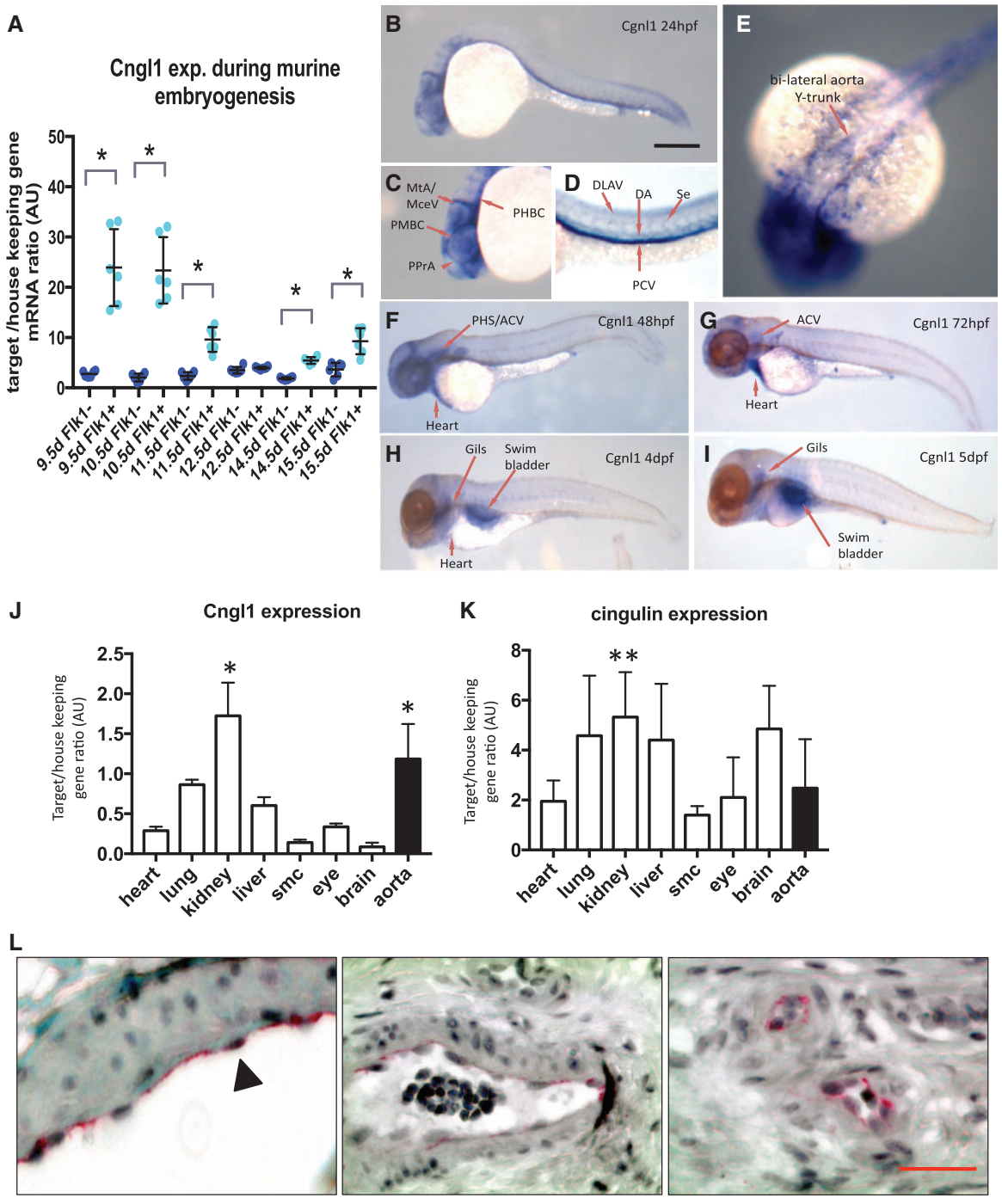

Figure 1 Cgnl1 is mainly expressed in vascular ECs. (*A*) Cgnl1 expression in Flk1+ and Flk1- cells during embryonic development of C57/bl6 mice from 9.5 to 15.5 days post-coital analyzed by qPCR. Mean ± SD, $n = 6$ for each time point, $^{*}P < 0.05$ versus time point matched Flk1- cells. Student's *t*-test. (*B*) Whole-mount *in situ* hybridization of wild type zebrafish larvae at different time points. Scale bar represents 5 mm. Lateral view: Cgnl1 targeting antisense probe signal (blue) detected in the vasculature at 24 hpf. (*C*) Cgnl1 expression is visible in the cranial vessels, including the middle cerebral vein, metencephalic artery, primordial midbrain channel, primitive prosencephalic artery, and primordial hindbrain channel. (*D*) In the trunk region, Cgnl1 signal is in the posterior cardinal vein, dorsal longitudinal anastomotic vessel, DA, and intersegmental vessel (Se). (*E*) Dorsal view: Expression of Cgnl1 in the bilateral aorta Y-trunk. (*F*) Regression of Cgnl1 signal during larvae maturation: Lateral view: Cgnl1 expression at 48 hpf is mainly located in cranial vessels, primary head sinus and anterior cardinal vein (ACV), and heart region. (*G*) Cgnl1 expression at 72 hpf is still detected in the ACV, and remains visible in the heart, whereas expression of Cgnl1 at (*H*) 4 dpf and (*I*) 5 dpf is mainly in the gills and swimbladder. QPCR analysis of (*J*) Cgnl1 and (*K*) cingulin expression in various tissues of mature C57/bl6 mice. Mean ± SD, $n = 5$, $^{*}P < 0.05$ aorta or kidney versus expression in all other tissues. $^{**}P < 0.05$ kidney versus expression in skeletal muscle. One-way ANOVA, followed by post hoc test with aorta or kidney set as control. (*L*) Immunostaining of Cgnl1 in human paraffin sections: From left to right, Cgnl1 expression is observed in the endothelium of macrovessels (first and second micrograph, indicated by black arrowhead) and microvessels (third micrograph). Scale bar represents 50 µm. Red signal, VEGFR2 immuno-staining; black, nucleus staining.

of one to three cells within 18 h, after which this initial network disintegrates due to the lack of stabilizing cues. Using siRNA that targeted endogenous Cgnl1 (siCgnl1) and scrambled siRNA as controls (sisham) in human primary HUVECs, the effect of Cgnl1 silencing on angiogenic sprouting potential was investigated.

SiCgnl1 transfection significantly reduced endogenous Cgnl1 mRNA and protein levels as compared with sisham-transfected and non-transfected (control) HUVECs (see Supplementary material online, *Figure S2A–D*). In addition, siRNA targeting of Cgnl1 did not affect family member cingulin on either protein or mRNA level (see Supplementary material online, *Figure S2E and F*). Quantitative comparison between siCgnl1-transfected and sisham-transfected cells showed no difference in sprouting capacity in the 2D-matrigel assay (see Supplementary material online, *Figure S2G and H*).

As Cgnl1 did not seem to affect initial vascular sprouting, we proceeded to study Cgnl1 function in vascular tubule construction in the presence of mural cells that provide vascular stabilizing cues. Tubule formation experiments were conducted in a well-validated 3D collagen type I gel coculture system. In this assay, GFP marked HUVECs are cocultured with RFP labelled pericytes to enable assessment of a number of critical steps, including assembly of multicellular, lumenized branching vessels. The multicellular nature of neovessels obtained with this 3D coculture assay is demonstrated in Supplementary material online, *Figure S3A* and *B*, and is shown in a time lapse movie (see Supplementary material online *Movie S1*). The effect of Cgnl1 silencing by siRNA targeting in HUVEC was assessed at Days 2 and 5 (*Figure 2A* and *B*, and see Supplementary material online, *Figure S3C*). Cgnl1 silencing (siRNA set 1) severely impeded the formation of new tubule structures as compared with non-transfected and sisham-transfected controls (*Figure 2B*). These results were further confirmed by using a second set of siRNA that targets Cgnl1 on different sequences (*Figure 2C* and *D*). In contrast, monocultures of HUVECs in 3D collagen matrix did not affect new tubule formation, indicating that pericyte interaction with ECs is important for the process of Cgnl1-mediated tubule formation (see Supplementary material online, *Figure S4A–D*). Cgnl1 expression was significantly upregulated in HUVECs that were cocultured with mural cells [vascular smooth muscle cells (VSMCs) or pericytes] as compared with HUVECs monocultures (see Supplementary material online, *Figure S4E*). Evaluation of the expression profile of the HUVECs in coculture with pericytes revealed that downregulation of Cgnl1 in HUVECs diminished Angiopoietin 1 (Angpt1) and increased VEGFA expression, whereas VEGFR2, Angiopoietin 2, Tie1, and Tie2 expression levels remained unaffected (see Supplementary material online, *Figure S4F*). In contrast, western blot analysis revealed no significant effect of Cgnl1 silencing on VEGFA and Angpt1 protein levels (see Supplementary material online, *Figure S4G*). Cgnl1 silencing in HUVECs did not affect pericyte numbers (see Supplementary material online, *Figure S5A*). Next, we assessed if induction of Cgnl1 expression in HUVECs is induced either by direct cell contact or paracrine stimulation by pericytes. HUVECs cultured on a thin porous membrane with direct contact of pericytes that are cultured on the other side show enhanced Cgnl1 expression versus HUVECs cultured without pericyte direct contact (see Supplementary material online, *Figure S5B* and *C*). In contrast, HUVECs cultured in the bottom well of a thin porous membrane insert in which percytes were seeded, allowing paracrine stimulation of HUVECs without direct pericyte contact, did not enhance Cngl1 expression versus HUVECs cultured in a similar setup without pericytes (see Supplementary material online, *Figure S5D*) These data indicate that induction of Cgnl1 expression in HUVECs in response to pericytes is mediated via direct contact between the two cell types. EC and pericyte interaction can take place in peg-and-socket contacts via (CX43-mediated) gap and (N-cadherin-based) adherence junctions.[16] To further investigate via which interaction mechanism pericyte activation of Cngl1 in ECs is mediated, we evaluated Cngl1 expression in HUVECs in response to pericyte direct contact stimulation with siRNA mediated knockdown of CXC43 and N-cadherin. Silencing of these peg-and-socket enriched proteins in HUVECs and pericytes did not affect induction of Cgnl1 expression in HUVECs by pericyte contact (see Supplementary material online, *Figure S5E* and *F*). Recent findings also indicate ECs and mural cells communicate via cross-cell type Notch ligand presentation,[17–19] initiating Notch signalling that promotes strong cell–cell contacts by Ve-cadherin immobalization at adherens junctions.[18–20] Indeed, siRNA mediated silencing of Notch1 and Notch4 and DLL4 in HUVECs and pericytes abolished Cgnl1 mRNA upregulation mediated by pericyte coculture (see Supplementary material online, *Figure S5G–I*). These data demonstrate that Cngl1 expression in ECs is enhanced via direct contact with pericytes via Notch signalling between the two cell types.

3.3 Cgnl1 silencing *in vivo* impedes retinal vasculature development in postnatal mice

To assess the *in vivo* relevance of these findings, the effect of Cgnl1 knockdown was studied in the developing retinal vasculature of postnatal C57/bl6 wildtype mice. Cgnl1 was silenced by injection of murine Cgnl1 targeting siRNA in the left and non-targeting siRNA in the right eye of 2-day-old pups. Injection of the non-targeting siRNA sequences did not affect retinal vascularization (data not shown). Silencing of Cgnl1 was verified by qPCR and western blot (see Supplementary material online, *Figure S6A* and *B*). At Day 6, the retinas were dissected and the vasculature was visualized by isolectin IB4 staining. Expansion of the vascular network from the neural plexus towards the retinal borders was impeded by Cgnl1 knockdown (*Figure 3A*). Assessment on higher magnification showed frequent malformation in the vascular structures and lower vessel density in siCgnl1 treated retinas (*Figure 3A*). Quantification of the vasculature showed decline in the number of vascular tubules, junctions, and in total tubule length (*Figure 3B*). Likewise, Cgnl1 silencing during a later timeframe (with injection at Day 8 after birth, during which a high density vascular network is well-established) compromised integrity of the vascular network, and further quantification showed a similar reduction in the number of tubules, junctions, and total tubule length at Day 12 (*Figure 3A* and see Supplementary material online, *Figure S6C*).

3.4 Cgnl1 silencing affects Rac1 and RhoA activity and decreases actin cytoskeleton assembly

It was previously reported that Cgnl1 is involved in the regulation of Rho-family GTPases activity in epithelial kidney cells.[12] Consequently, we assessed RhoA, cdc42 and Rac1 activities using ELISA-based activity assays. HUVECs were seeded on a thin layer of gelatin/collagen coating to provide an integrin-ECM contact trigger for GTPase activation, and were harvested after 20 and 40 min of stimulation for analysis. Cgnl1 silencing in HUVECs significantly reduced Rac1 activation early after cell seeding (*Figure 4A*), whereas RhoA activity was increased (*Figure 4A*). In contrast, no significant effect was observed in the activation of the small GTPase cdc42 in comparison to sisham-transfected controls (*Figure 4A*). Western blot analysis showed no difference in total Rac1, RhoA and cdc42 protein levels (see Supplementary material online, *Figure S7A*). In line with the observation that Cgnl1 expression is increased in HUVECs

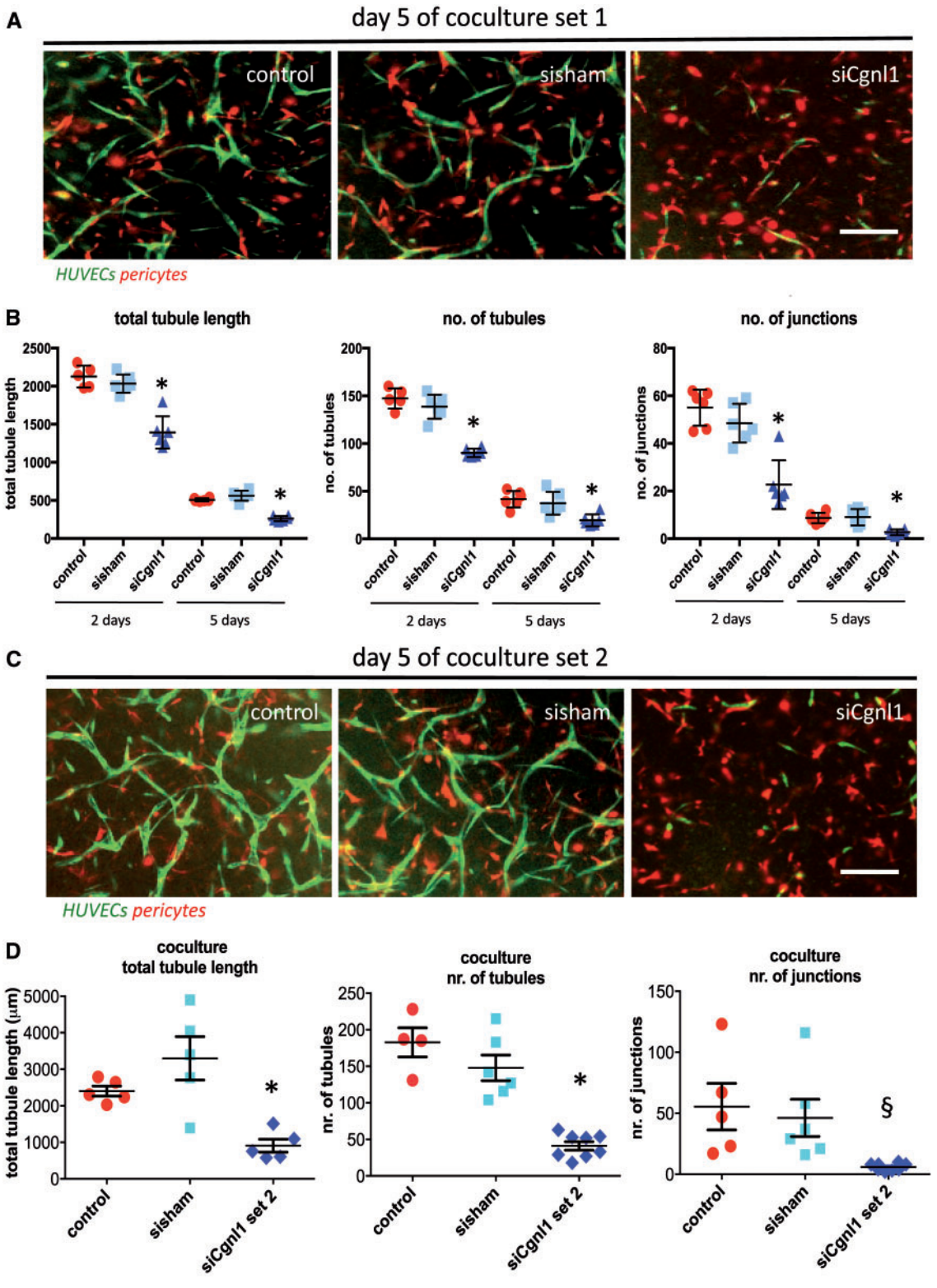

Figure 2 Cgnl1 knockdown impairs vascular network stabilization *in vitro*. (*A*) Representative results at Day 5 in 3D collagen matrix coculture following Cgnl1 silencing or sham siRNA transfection in HUVEC-GFP (green). Pericytes are marked by RPF (red). Scale bars in (A) and (C) represent 100 µm. (*B*) Quantitative analysis shows the number of total tubule length, and number of tubules and junctions in coculture conditions ($n = 5$). Values represent means ± SD. *$P < 0.05$ siCgnl1 versus time-corresponding control and sisham. Black bars indicate 2 days and white bars indicate data of 5 days coculture. One-way ANOVA for comparisons within one time point. (*C*) Representative results at Day 5 in 3D collagen matrix coculture following Cgnl1 silencing with siRNA Set 2. (*D*) Data of quantified coculture conditions at Day 5, following silencing with Cngl1 targeting siRNA set 2 ($n > 5$). Values represent means ± SD, *$P < 0.05$, §$P < 0.1$, siCgnl1 versus time-corresponding control and sisham. One-way ANOVA for comparisons within one time point.

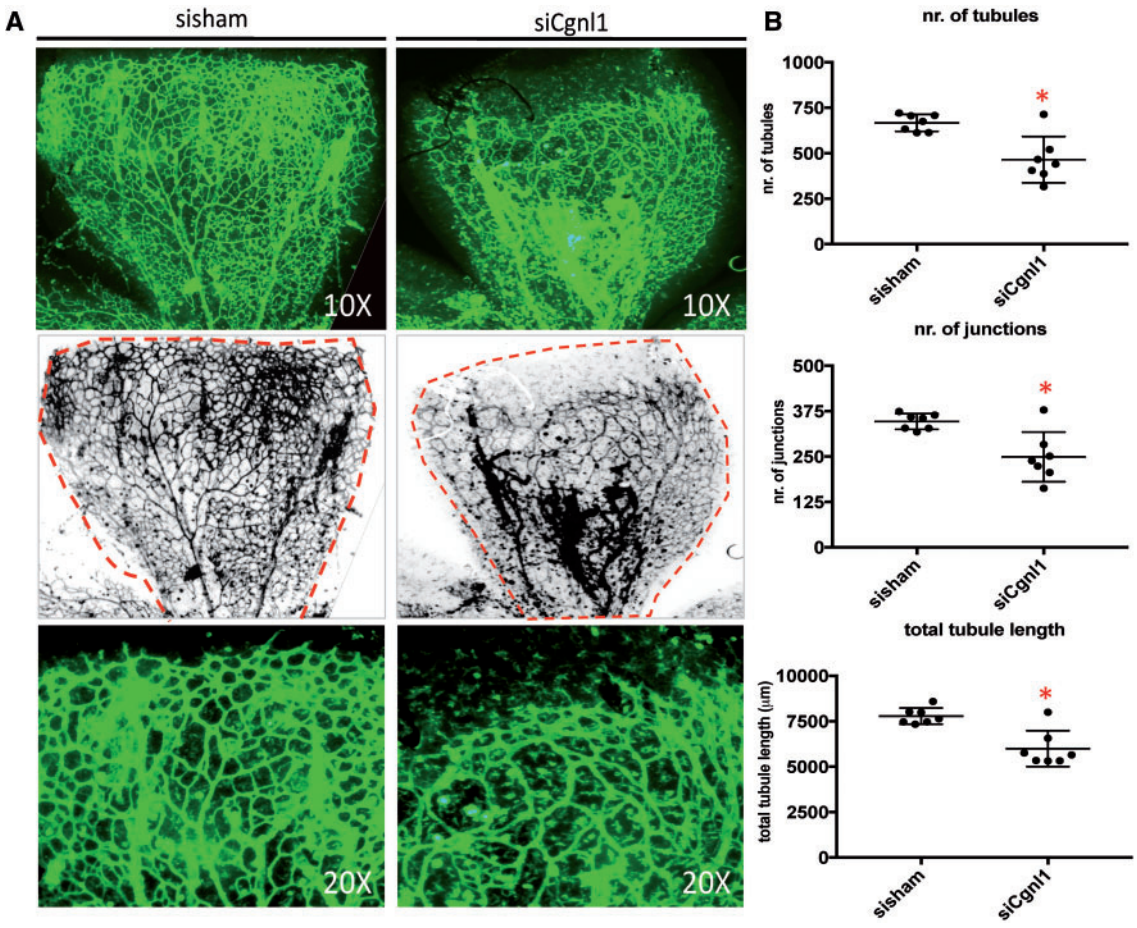

Figure 3 Cgnl1 silencing impedes vasculature development *in vivo*. (*A*) Top row of images show representative micrographs of the developing retinal vasculature visualized by whole mount isolectin IB4 staining (FITC signal) at Day 6. Second row of images show inverted version of micrographs used for quantification, red broken lines indicate retinal borders. 10× magnification. Third row of images show high magnification micrographs of the angiogenic front. 20× magnification. (*B*) Quantified results of retinal vascularization at Day 6 after siCgnl1 injection at Day 2 as compared with sisham-injected controls. Mean ± SD per group is indicated in scatter plots. *$P < 0.05$ versus sisham-injected eyes ($n = 7$ pups per group). Student's *t*-test.

in response to pericyte stimulation, HUVECs cocultured with pericytes showed a significant increase in Rac1 activation versus single culture HUVECs (see Supplementary material online, *Figure S7B*). In addition, silencing of Cngl1 in HUVECs abolished these effects of pericyte stimulation (see Supplementary material online, *Figure S7C*). Our data showed that upregulation of Cgnl1 expression by pericyte contact in HUVECs was mediated via Notch signalling. Indeed silencing of Notch4 abolished the effects on Rac1 activity by pericyte stimulation of HUVECs (see Supplementary material online, *Figure S7C*). These data demonstrate that Cngl1 upregulation in HUVECs by pericyte crosstalk with HUVECs via Notch signalling enhances endothelial Rac1 activity.

A delay in cell-morphological adaptation during adhesion of Cgnl1 silenced HUVECs implied that actin-cytoskeletal assembly in these cells was affected. To study this in more detail, siCgn1 and sisham transfected HUVECs were seeded on gelatin/collagen-coated glass slides, and morphological changes in the actin-cytoskeleton during cell adhesion were studied by phalloidin-Rhodamine staining at 10 and 20 min after seeding *Figure 4B*). Cgnl1 knockdown caused a delay in actin-adaptation, identified by a significant decrease in the number of cells with a distinct flat morphology with clear actin-distribution at the cell periphery, and an increased in rounded cells with limited actin redistribution after 10 min of adhesion (*Figure 4C*). To further validate these findings, live imaging was conducted in the previously described 3D collagen type I gel coculture system. Cellular adaptation of GFP marked HUVECs was monitored for up to 50 time points post-initiation of the assay (1 time point = 1 h). Silencing of Cgnl1 in HUVECs-GFP reduced the morphological adaptive capacity of these cells, shown by a significant reduction in the siCgnl1 treated group in natural increase of *aspect ratio* (AR = major axis/minor axis) per GFP+ structure as observed in sisham treated controls, indicating a defect in cell elongation (*Figure 4D* and *E*). Similarly, the natural decrease in *roundness* per GFP+ structure was significantly reduced in the siCngl1 treated group (*Figure 4D* and *E*). These results were further confirmed by using a second set of siRNA that targeted Cgnl1 on different sequences (see Supplementary material online, *Figure S7B*).

The observed effects of Cgnl1 silencing on neovessel formation could be caused by changes in EC proliferation or apoptosis. However, Cgnl1 silencing did not immediately affect EC proliferation, as shown by lack of difference in BRDU incorporation and cell cycle progression (see Supplementary material online, *Figure S8A* and *B*) between the sisham

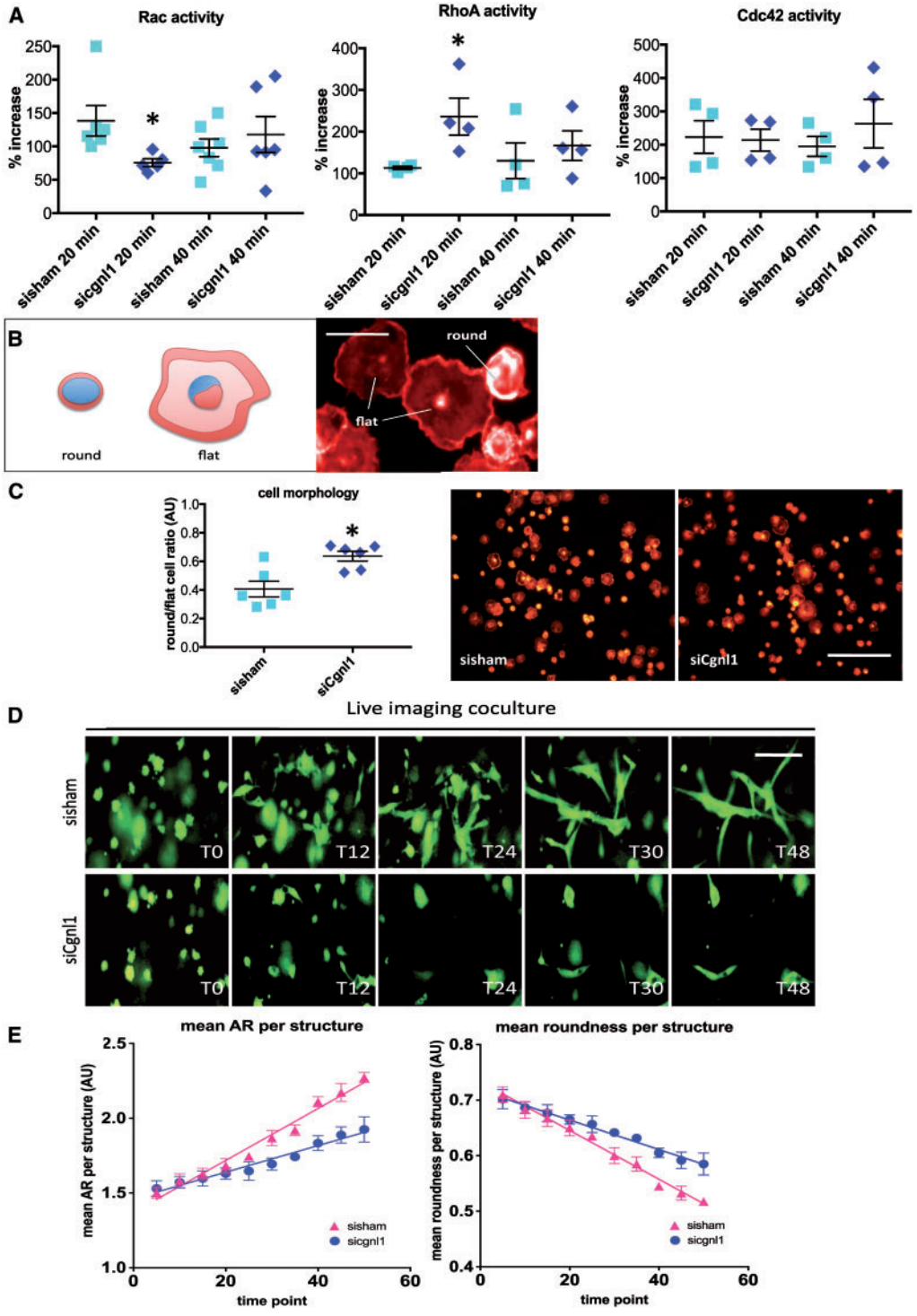

Figure 4 Cgnl1 regulates Rac1 and RhoA signalling and actin cytoskeleton dynamics. (*A*) Chemo-luminescence measurement of the GTP-bound small G-proteins in cell lysates from siCgnl1 or sisham-transfected HUVECs after 20 and 40 min of cell seeding, showing the levels of GTP-Rac1, GTP-Rho-A, and GTP-cdc42. Values represent means ± SD. *$P < 0.05$ versus sisham in corresponding time group ($n > 4$). Student's *t*-test. (*B*) Micrographs of typical results of a cell adhesion assay in which sisham and siCgnl1 treated HUVECs are seeded on a gelatine/collagen coated surface and analyzed for cell-spreading after 10 min adhesion. Scale bar represents 10 µm. (*C*) Actin visualized by phalloidine staining enables distinction between adherent cells (flat cell morphology) and non-adherent cells (round cell morphology). Scale bar represents 100 µm. Bargraph shows round/flat cell ratio in the siCgnl1 and sisham transfected groups. Values represent means ± SD. *$P < 0.05$ versus sisham in corresponding group ($n = 6$). Student's *t*-test. (D) Serial images of time-lapse imaging of HUVECs GFP cells seeded in 3D collagen coculture with pericytes in siCgnl1 and sisham group. Different time points (T) are shown. 1 time point represents 1-h post-seeding. Scale bar represents 50 µm. (*E*) Quantification of AR and roundness per HUVEC-GFP+ structure (from T = 0 to 50 post-seeding). Each symbol represents average ± SD of five time points. Each time point is composed of 5 individual measurements. $P < 0.0001$ for AR and roundness, siCngl1 versus sisham group, linear regression analysis, overall comparison.

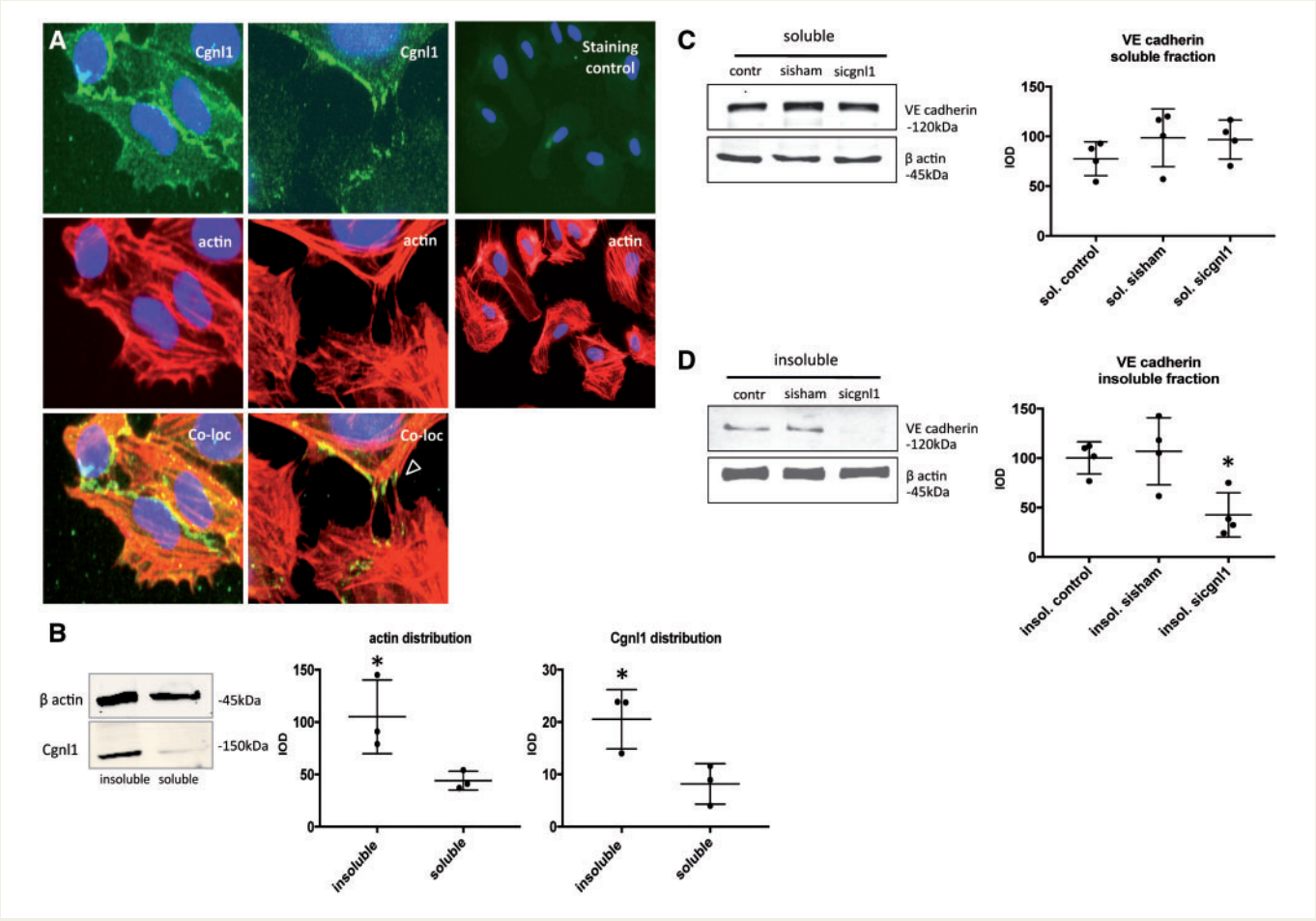

Figure 5 Cgnl1 silencing disrupts Ve-cadherin association with the actin cytoskeleton. (*A*) Intracellular staining of HUVECs for Cgnl1 (green signal), DAPI (blue signal) and actin cytoskeleton filaments (red signal), arrowhead indicates Cgnl1 signal colocalized with actin fibers in filopodia during interaction with neighbouring cells. Immunostaining using a species-matched isotypic control validated Cgnl1 signal specificity, as shown in the third column. Micrographs are depicted at 40 × (first two columns), and 20× magnification (third column) ($n = 4$). (*B*) Cgnl1 protein levels in HUVECs in the Triton-X insoluble fraction (the actin cytoskeleton associated compartment) versus the soluble fraction. Shown are representative Western blots for β actin and Cgnl1 (left). Graphs show quantified results (right). Values represent mean integrated optical density (IOD) ± SD corrected for β actin loading controls. *$P < 0.05$ versus soluble ($n = 3$). Student's *t*-test. (*C* and *D*) Western blot results show Ve-cadherin protein level in the Triton-X soluble and insoluble fraction in siCgnl1-treated confluent HUVEC monolayers versus sisham or non-treated controls. Graphs show quantified results. Values represent mean IOD ± SD corrected for β actin loading controls. *$P < 0.05$ versus sisham and control ($n = 4$). One-way ANOVA.

and siCgnl1 treated groups at 4 and 12 h post-cell cycle initiation respectively. In addition, PI/AnnexinV analysis by flow cytometry showed that Cgnl1 silencing in HUVECs *in vitro* did not affect EC apoptosis at 4 h post-cell cycle activation (see Supplementary material online, *Figure S8C*). Together, these data imply that the inhibitory effect of Cgnl1 silencing on vascular formation is not direct dependent on cell proliferation and apoptosis, but may be mediated by Rho-family GTPase regulation of cell morphology via modification of the cytoskeleton.

3.5 Cgnl1 silencing disrupts Ve-cadherin association with the actin cytoskeleton and impairs Ve-cadherin adherens junction stabilization

Co-localization of Cgnl1 with the actin cytoskeleton in kidney epithelial cells was previously reported. Here we assessed the intracellular localization of Cgnl1 in human ECs. Cgnl1 antibody staining showed co-localization of Cgnl1 with phalloidin-stained actin filaments in HUVEC cultures (*Figure 5A*). Protein association with the cytoskeleton can be evaluated by comparing the TritonX-100 insoluble with the TritonX-100 soluble fractions of cell extracts.[21] Comparison between the TritonX-100 soluble and insoluble compartment of confluent HUVEC cultures clearly showed a predominant presence of Cgnl1 in the Triton-X100 insoluble (cytoskeleton associated) fraction (*Figure 5B*). Soluble and insoluble fractions were adequately separated, as shown by predominant enrichment of VEGFA in the soluble fraction (see Supplementary material online, *Figure S9A*).

Cgnl1 was previously shown to affect adherence junction stability via Rac1 activation in kidney epithelial cells.[12] Actin cytoskeleton association with Ve-cadherin is crucial for adherens junction formation and survival of the neovasculature. Hence, we evaluated the levels of Ve-cadherin in endothelial soluble and insoluble fractions. No difference was observed

in the soluble fraction between the groups (*Figure 5C*). In contrast, Cgnl1 silencing in confluent HUVEC monolayers significantly reduced the level of Ve-cadherin protein in the Triton-X100 insoluble (actin cytoskeleton associated) fraction as compared with the controls (*Figure 5D*). Immunofluorescent microscopy revealed that Cgnl1 silencing affected Ve-cadherin localization at cell-cell contacts in confluent HUVEC monolayers *in vitro*. Thus, a significant decrease in Ve-cadherin+ adherens junction formation at the cell-cell borders was observed (*Figure 6A* and *B*). This decrease in Ve-cadherin recruitment at adherens junctions in the Cngl1 silenced condition was also observed when the confluent layer of HUVECs was in contact with mural cells (pericytes) (*Figure 6C* and *D*). These data indicate that Cgnl1 promotes Ve-cadherin adherens junctions formation in ECs.

3.6 Cgnl1 silencing impairs FAK signalling and focal adhesion complex assembly

Except for modulation of cell–cell junctions, Rac1 is a known key modulator of integrin-focal adhesion complex assembly, a process that plays a prominent role in EC morphological adaptation during tubule formation. Indeed activated (GTP bound) Rac1 was found to be recruited to initial focal adhesion sites.[22] As Cgnl1 modulates Rac1 activation, and EC adhesion was affected in Cgnl1 silenced HUVECs, we hypothesized that Cgnl1 may also affect focal adhesion complex assembly in response to EC–extracellular matrix (ECM) contact. We investigated the effect of Cgnl1 silencing on focal adhesion-assembly in the response to cell–ECM interaction. Immunofluorescent intracellular staining was conducted on siCgnl1 or sisham treated HUVECs at 30, 60, and 120 min after seeding on gelatin/collagen coated glass slides. A significant defect in assembly of focal adhesion-structural proteins paxillin and vinculin (*Figure 7C–F*) were observed in Cgnl1 silenced HUVECs at 60-min post-seeding as compared with sisham controls (*Figure 7C–F*). Recruitment and activation of FAK at nascent focal adhesion sites is required to strengthen and maturate the focal adhesion complex. Intracellular staining revealed that Cgnl1 silencing inhibited FAK recruitment at focal adhesion sites at 30, 60 and 120 min post-seeding (*Figure 7A* and *B*). This decrease in focal adhesion assembly in Cgnl1 silenced condition was also observed when the confluent layer of HUVECs was cultured in contact with mural cells (pericytes) (see Supplementary material online, *Figure S9B* and *C*), as shown by paxillin analysis.

Western blot analysis also showed a significant decrease in vinculin, but not paxillin protein levels (see Supplementary material online, *Figure S9D*), indicating that the effects observed for vinculin may be directly linked to a reduction in vinculin protein. Western blot analysis showed no changes in total FAK protein levels in Cgnl1 silenced ECs (see Supplementary material online, *Figure S9E*). In contrast, a decline in phospho-Y397-FAK levels in siCgnl1-treated cells compared with sisham-treated controls was observed at 20 min after seeding (*Figure 7G*), indicative of a reduction in FAK activation. Downstream activation of C-Src was impeded by Cgnl1 knockdown as well, shown by a decrease in phospho-Y418-C-Src at 40 min post-seeding, whereas total C-Src remained unaffected (*Figure 7H* and see Supplementary material online, *Figure S9E*). Combined, these data indicate that Cgnl1 silencing in ECs diminishes focal adhesion assembly and FAK signalling in response to EC–ECM contact. These perturbations in the basic pathways of cell morphological adaption, in addition to the observed diminished assembly of Ve-cadherin adherens junctions, could induce instability of neovasculature and negatively affect the capacity of neovessels for further growth. To evaluate this concept, time lapse live imaging was conducted in the 3D collagen type I gel coculture system. GFP+ vascular structures were monitored for up to 125 time points post initiation of the assay (1 time point = 1 hour). Although in the early time points (<25 time points/h), no difference in area per GFP+ structure between siCngl1 and sisham groups was observed, silencing of Cgnl1 in HUVECs-GFP at later time points (>25 time points/h) significantly reduced the natural size increase per GFP+ vascular structure that was observed in sisham coculture conditions, indicating reduced tubule stability (*Figure 7I* and *J*). Finally, these results were further confirmed by using a second set of siRNA that targeted Cgnl1 on different sequences (see Supplementary material online, *Figure S9F*).

4. Discussion

In this study we report several findings: (i) Unlike cingulin, Cgnl1 expression is mainly enriched in ECs during vascular growth. (ii) Cgnl1 is pivotal for stable tubule structure formation during new vessel formation, as shown *in vitro* using loss-of function studies in a 3D matrix co-culture system that uses primary human ECs and supporting mural cells. (iii) Cgnl1 is critical for vascular growth *in vivo*, as shown in the murine retina vascularization model. (iv) Cgnl1 in ECs promotes Ve-cadherin association with the actin cytoskeleton and induces adherens junction stabilization. (v) Cgnl1 promotes focal adhesion assembly in response to ECs–ECM contact. To our knowledge this is the first study to identify Cgnl1 as an important regulator of new vessel formation both *in vitro* and *in vivo*. It also provides new evidence for the involvement of Cngl1 in the regulation of Ve-cadherin assembly at adherens junctions in ECs.

4.1 High level of expression of Cgnl1 in ECs

Cgnl1 was reported to be highly expressed in renal epithelial cells.[12,23] We detected significant higher Cgnl1 expression levels in Flk1+ (ECs) versus Flk1- (non-ECs) at different stages of mouse embryo development. Using *in situ* hybridization we showed that Cngl1 expression in developing zebrafish larvae is mainly observed in vascular structures. In human bloodvessels, we detected a strong endothelial Cngl1 signal by immunochemistry. Our observations are in line with the findings of Narumiya *et al.*,[13] who reported that Cgnl1 was highly expressed in CD31+ (endothelial) cells in mouse embryos on embryonic day (E)8.5 and E9.5. These data imply a role for Cngl1 in the regulation of EC function.

4.2 Cgnl1 regulates stable tubule structure formation and proves crucial for *in vitro* and *in vivo* angiogenesis

Cgnl1 has been implicated to be involved in the regulation of EC junctions: In a study focussed on the regulation of ZO-1 in cultured human dermal microvascular cells (HDMEC), Tornavaca *et al.*[15] reported that Cgnl1 was located at tight junctions of confluent HDMEC monolayers. ZO-1 silencing in HDMECs led to reduced localization at tight junctions of Cngl1, whereas Cngl1 silencing led to redistribution of vinculin from cell junctions to focal adhesions and promoted stress fibers formation. ZO-1 and p114rhoGEF were shown to co-immunoprecipitate with Cgnl1, indicating direct binding between these proteins. Combined, the data of Tornavaca *et al.* indicate that p114RhoGEF together with ZO-1 and Cngl1 stimulate junctional actomyosin activation, leading to coupling of mechanotransducers to the tight junction complex, thereby ensuring barrier function of the endothelium. However, no direct evidence was

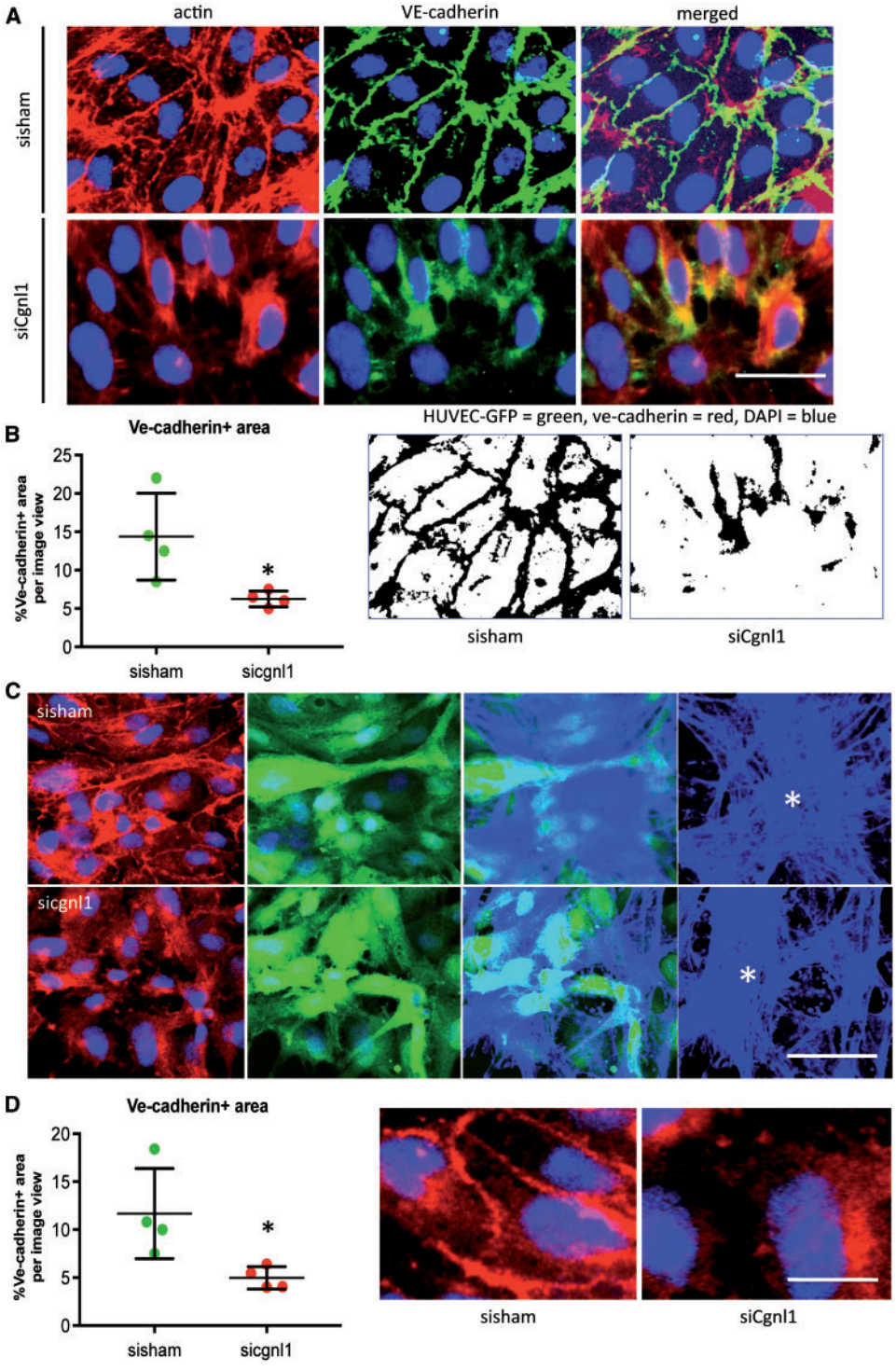

Figure 6 Cgnl1 silencing impairs Ve-cadherin adherens junction stabilization. (*A*) Representative micrographs of fluorescent immunostaining for actin (red) and Ve-cadherin (green) distribution in confluent HUVEC monolayers treated with set 1 siCngl1 versus sisham control. Scale bar represents 10 μm. (*B*) Quantification analysis of percentage of the Ve-cadherin+ area at cell junctions. Values represent means ± SD. *$P < 0.05$ versus sisham. Images (right) show inverted version of micrographs used for quantification. Data obtained from four different experiments, with analysis of 12 different micrographs per group per experiment. One-way ANOVA. (*C*) Representative micrographs of z stack analysis of HUVEC-GFP culture on top of pericyte-RFP, showing the fluorescent signal of Ve-cadherin (shown in red, first column) in confluent HUVEC-GFP + (GFP shown in green, second column) layer treated with siCngl1 versus sisham. DAPI signal in blue. Third column shows composite images of the phalloidin blue + (Alexa Fluor 350) pericyte layer beneath the HUVECs-GFP (green). Last column shows isolated Z-stack layer of phalloidin blue+ pericytes (asterisk indicated). Scale bar represents 20 μm. (*D*) Quantification analysis of percentage of the Ve-cadherin+ area at cell junctions. Values represent means ± SD. *$P < 0.05$ versus sisham and control. Images (right) show high details of Ve-cadherin at adherens junctions. Scale bar represents 5 μm. Data obtained from four different experiments, with analysis of six different micrographs per group per experiment. One-way ANOVA.

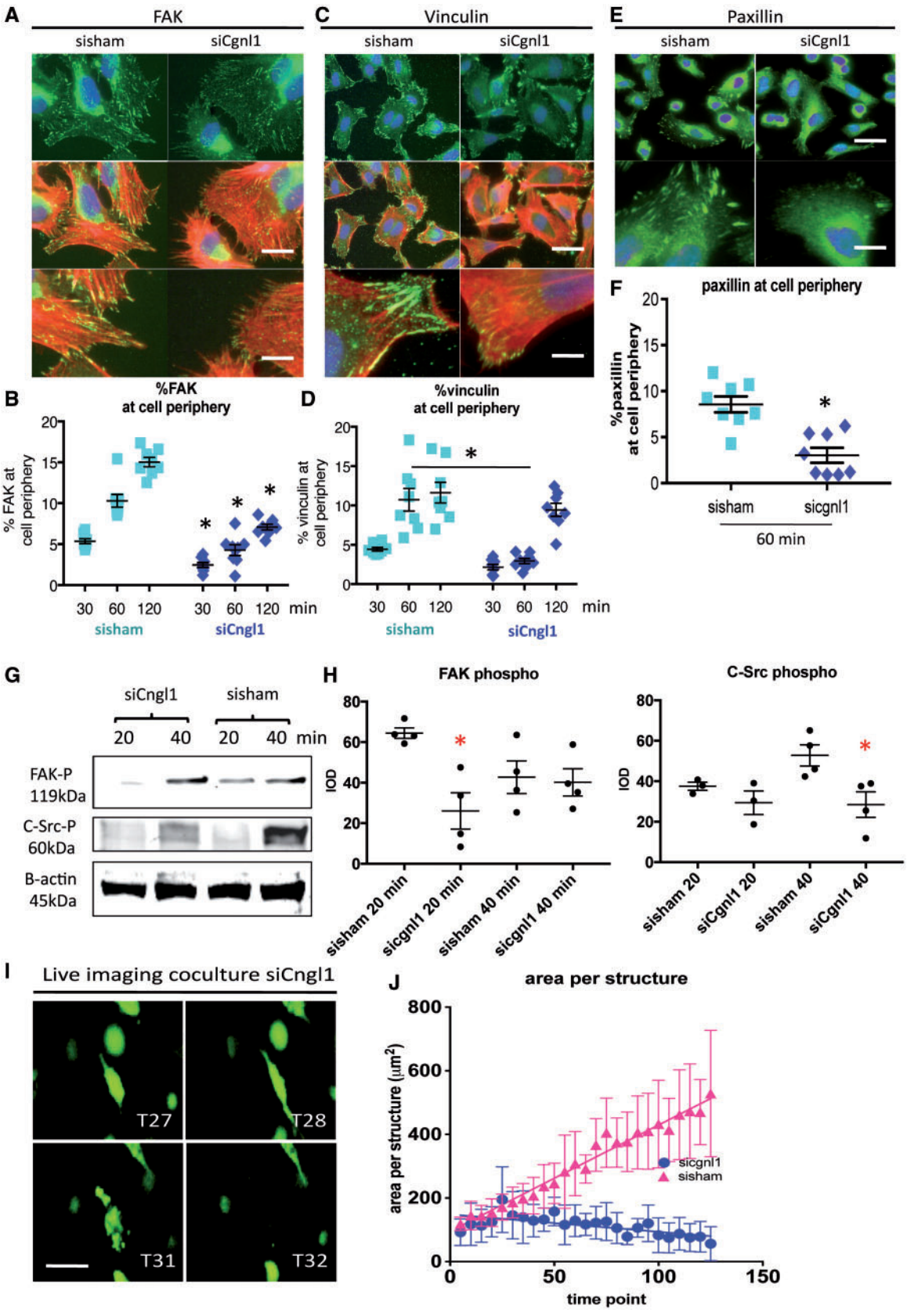

Figure 7 Cgnl1 inhibition hampers focal adhesion site assembly. Representative micrographs of intracellular immunostaining in HUVECs for (*A*) focal adhesion signalling protein FAK (FITC) and the actin cytoskeleton (Phalloidin Rhodamine), for focal adhesion proteins (*C*) vinculin and (*E*) paxillin, in sisham and siCgnl1 tranfected HUVECs after 1 h of adhesion to a gelatin/collagen coated underground. DAPI (blue signal). Upper two rows: Scale bar represents 5 µm. Lower rows show high magnification details. Scale bar represents 2 µm. Quantitative results of (*B*) %FAK, (*D*) % vinculin, and (*F*) %paxillin distribution

provided to demonstrate a role for cngl1 in the process of angiogenesis, and in particular tubule structure formation.

In our study, we provide for the first time both *in vitro* (3D coculture assay) and *in vivo data* (murine retina vascularization model) that demonstrate that Cgnl1 silencing significantly inhibits the angiogenic capacity of vascular cells. Cgnl1 silencing greatly impaired tubule structure formation in the 3D coculture assay, and diminished the number of vascular structures formed during vascular expansion in the developing retina.

4.3 Cgnl1 in ECs promotes Ve-cadherin association with the actin cytoskeleton and induces adherens junction stabilization

The molecular mechanism of Cgnl1 has been mainly investigated *in vitro* in epithelial kidney cells, although it has also been shown in cultured urotherial cells that expression levels of Cngl1 is tightly regulated by miR-205.[24] In renal epithelial cells, Cgnl1 was identified as a cell-cell junctional complex adaptor protein.[10,12] After recruitment of Cngnl1 to the tight junctions via ZO-1, Cgnl1 promotes Rac1 activation via Tiam1, and inhibits RhoA activity by GEFH1 inhibition.[12] Other studies have also indicated that Cgnl1 localizes in adherens junctions.[10,25] Only one study reported the function of Cngl1 in vascular endothelial cells (HDMECs). Similar to the findings in epithelial kidney cells, this study in HDMECs demonstrated a regulatory role for ZO-1 in tight junction recruitment of Cgnl1.[15]

In our study, we focused on the regulation of Cgnl1 of adherens junctions via GTPases and actomyosin regulation. In line with the findings in renal epithelial cells, our data showed that Cgnl1 silencing in HUVECs inhibited Rac1 and promoted RhoA activity respectively, which led to impaired Ve-cadherin colocalization with actin filaments at adherens junction sites. The actin cytoskeleton at the cell periphery is composed of a highly organized meshwork of filamentous actin, which is closely associated with the nearby plasma membrane with cell–cell junction and ECM–cell focal adhesion complexes. Intracellular Cgnl1 co-localized with actin filaments,[10,12] and Cgnl1 knockdown delayed cadherin recruitment and subsequent adherens junction assembly in epithelial cells. Our findings demonstrate that Cgnl1 is co-localized with the actin cytoskeleton and is enriched in the Triton-X100 insoluble (actin cytoskeleton-associated) fraction in ECs. Knockdown of Cgnl1 induced Ve-cadherin-actin dissociation, implied by a decline in Ve-cadherin in the Triton-X100 insoluble compartment, and a decrease in Ve-cadherin accumulation at adherens junction sites. Combined with previous reported findings, the data demonstrate that Cgnl1 could affect vascular growth by promoting adherens junction stabilization.

4.4 Cgnl1 promotes focal adhesion assembly in response to ECs–ECM contact

Focal adhesions are dynamic protein complexes that provide a linkage point between the cells extra- and intra-cellular environment, playing a central role in migration and cell adhesion.[26,27] Rac1 deletion significantly inhibited focal adhesion assembly in mouse embryonic fibroblasts, whereas overexpression of an active RhoA mutant failed to rescue the observed phenotype.[26] In a transgenic mouse model, expression of a constitutively active form of Rac1 altered focal adhesion structures.[28] The previous study in HDMECs demonstrated a regulatory role of Cgnl1 in vinculin distribution to focal adhesions. In line with these observations, our study showed that Cgnl1 silencing impaired focal adhesion assembly, coinciding with a reduction in Rac1 activation.

4.5 Proposed mechanism for Cngl1 in neovessel formation

Based on our findings on the important role for Cgnl1 in vessel formation, we hypothesize that the main function of Cgnl1 during vascular growth is tubule formation by control of adherens junction and focal adhesion assembly via regulation of Rac1 activity. Initial contacts between ECs are relatively weak, with serrated Ve-cadherin junctions, providing ECs with high motility to respond to e.g. VEGFA gradients.[20,29] In contrast, Notch signalling, provided either by neighbouring endothelial tip cells, or by pericytes via Notch ligand presentation, has been shown to promote the formation of strong cell–cell contacts with immobile straight Ve-cadherin junctions, that limit the migration capacity of the connected cells.[18,20,29] Based on our (live imaging) findings, which highlight the inhibitory effects of siCgnl1 on the capacity of ECs to undergo stable morphological adaptations to form and extend 3D neo tubule structures, Cngl1 could be mainly involved in the formation of strong Ve-cadherin junctions that promote immobile cell–cell connections in response to Notch signalling provided by pericytes, while it has a limited impact on initial weak (Ve-cadherin) bond formation. Indeed, our data demonstrate that Cngl1 expression in HUVECs is significantly enhanced by direct cell contact with pericytes. Furthermore, this induction of Cgnl1 expression in HUVECs is facilitated via Notch signalling, as knockdown of Notch1/4 and DLL4 in both cell types severely impeded the Cgnl1 induction in HUVECs in response to pericyte stimulation. Our data further demonstrate that Cngl1 upregulation in HUVECs by Notch signalling with pericytes enhances endothelial Rac1 activity. In further support of this concept, our analysis of the time lapse data indeed reveals that siCngl1 structures are more instable compared with sisham structures, negatively affecting the capacity of the individual neovessels for elongation beyond the two to three cell stage.

Thus, based on our current findings, we propose a working mechanism for Cngl1 in which pericyte-induced upregulation of Cngl1 in ECs via Notch signalling promotes the formation of strong Ve-cadherin adherens junctions via Rac1 activation. Simultaneously, Cngl1 mediated Rac1 activation stimulates assembly of integrins-focal adhesion complexes. Combined, formation of both strong adherens junctions and focal

at cell borders per image view adjusted for cell numbers at different time points of the adhesion assay. Values represent means ± SD. *$P < 0.05$ versus time point matched sisham conditions. Data obtained from 8 different experiments with analysis of 12 different micrographs per group per experiment. Two-way ANOVA. Western blot analysis at 20 and 40 min after seeding of (*G*) FAK-phospho-Y397 and (*H*) C-Src-phospho-Y418 proteins level in siCgnl1-treated HUVECs compared with control groups. Quantified values in graph are shown in mean IOD ± SD corrected for β actin loading controls. *$P < 0.05$ versus sisham and control of corresponding time points ($n = 3–4$). Student's t-test for comparison within 1 time point. β actin protein level was assessed as a loading control and did not differ between the control, sisham and siCgnl1 samples (data not shown). (*I*) Serial images of time-lapse imaging of HUVECs GFP cells seeded in 3D collagen coculture with pericytes in siCgnl1 group. Different time points (T) are shown. 1 time point represents 1 hour post seeding. Scalebar represents 10 μm. (J) Quantification of area per HUVEC-GFP+ structure (from T = 0 to 125 post-seeding). Each symbol represents average area per structure ± SD of five time points. Each time point is composed of five individual measurements. $P < 0.0001$, siCngl1 versus sisham group, linear regression analysis, overall comparison.

adhesions ensures stabilization and further elongation of neovascular tubules (see Supplementary material online, *Figure S10*).

4.6 Limitations of the study

The use of siRNA to target Cgnl1 in the murine retinal vascularization model evokes a mild influx of IB4-possitive immune cells that may affect vascular growth. To be able to make a distinction between the effects that are the result of Cgnl1 inhibition and the effects that are linked to the use of siRNA, we injected the control retinas with a set of non-targeting siRNAs. As we compared non-targeting siRNA with Cgnl1 targeting siRNA-treated conditions, we consider the observed vascular phenotype, at least in part, to be the direct result of Cngl1 silencing, and not merely a side effect of immune cells activation by siRNA treatment itself. However, it cannot be entirely excluded that the observed effects of Cngl1 silencing in the murine retina model may have been facilitated by a background of increased immune activation. Although the Triton-X lysate separation method could help to distinguish soluble and insoluble fractions, our data set only provides evidence that Cngl1 is enriched in the same insoluble fraction as cytoskeletal actin, and does not show direct binding between Cngl1 and actin protein.

5. Conclusions

Cgnl1 mediates vascular growth by stabilizing newly formed vascular tubules via adherens junction stabilization in ECs. Stimulation of neovessels by recruited pericytes via cross-cell type Notch signaling enhances the Cgnl1-mediated stabilization process in ECs. Our findings support an important function of Cgnl1 in regulation of vascular growth during embryonic development and vascular-related disease in adulthood.

Supplementary material

Supplementary material is available at *Cardiovascular Research* online.

Acknowledgements

The authors would like to thank Mariëlle Maas, Hans Meijer, and Mikel Rijken for expert technical assistance.

Conflict of interest: none declared.

Funding

This work was funded by grants from the Dutch Organization for Scientific Research (grant 91776325 to H.J.D., and grant 91696061 and 91714302 to C.C.), the EMC fellowship grant (C.C.) and UMCU RM fellowship grant (C.C.).

References

1. Carmeliet P. Angiogenesis in life, disease and medicine. *Nature* 2005;**438**:932–936.
2. Jain RK. Molecular regulation of vessel maturation. *Nat Med* 2003;**9**:685–693.
3. Spindler V, Schlegel N, Waschke J. Role of GTPases in control of microvascular permeability. *Cardiovasc Res* 2010;**87**:243–253.
4. Fryer BH, Field J. Rho, Rac, Pak and angiogenesis: old roles and newly identified responsibilities in endothelial cells. *Cancer Lett* 2005;**229**:13–23.
5. Heasman SJ, Ridley AJ. Mammalian Rho GTPases: new insights into their functions from in vivo studies. *Nat Rev Mol Cell Biol* 2008;**9**:690–701.
6. Tan W, Palmby TR, Gavard J, Amornphimoltham P, Zheng Y, Gutkind JS. An essential role for Rac1 in endothelial cell function and vascular development. *faseb J* 2008;**22**:1829–1838.
7. Dejana E, Orsenigo F, Lampugnani MG. The role of adherens junctions and VE-cadherin in the control of vascular permeability. *J Cell Sci* 2008;**121**:2115–2122.
8. Lampugnani MG, Dejana E. Adherens junctions in endothelial cells regulate vessel maintenance and angiogenesis. *Thromb Res* 2007;**120**:S1–S6.
9. Hall A. Rho GTPases and the control of cell behaviour. *Biochem Soc Trans* 2005;**33**:891–895.
10. Guillemot L, Guerrera D, Spadaro D, Tapia R, Jond L, Citi S. MgcRacGAP interacts with cingulin and paracingulin to regulate Rac1 activation and development of the tight junction barrier during epithelial junction assembly. *Mol Biol Cell* 2014;**25**:1995–2005.
11. Guillemot L, Schneider Y, Brun P, Castagliuolo I, Pizzuti D, Martines D, Jond L, Bongiovanni M, Citi S. Cingulin is dispensable for epithelial barrier function and tight junction structure, and plays a role in the control of claudin-2 expression and response to duodenal mucosa injury. *J Cell Sci* 2012;**125**:5005–5014.
12. Guillemot L, Paschoud S, Jond L, Foglia A, Citi S. Paracingulin regulates the activity of Rac1 and RhoA GTPases by recruiting Tiam1 and GEF-H1 to epithelial junctions. *Mol Biol Cell* 2008;**19**:4442–4453.
13. Narumiya H, Hidaka K, Shirai M, Terami H, Aburatani H, Morisaki T. Endocardiogenesis in embryoid bodies: novel markers identified by gene expression profiling. *Biochem Biophys Res Commun* 2007;**357**:896–902.
14. Cheng C, Haasdijk R, Tempel D, van de Kamp EH, Herpers R, Bos F, Den Dekker WK, Blonden LA, de Jong R, Burgisser PE, Chrifi I, Biessen EA, Dimmeler S, Schulte-Merker S, Duckers HJ. Endothelial cell-specific FGD5 involvement in vascular pruning defines neovessel fate in mice. *Circulation* 2012;**125**:3142–3158.
15. Tornavaca O, Chia M, Dufton N, Almagro LO, Conway DE, Randi AM, Schwartz MA, Matter K, Balda MS. ZO-1 controls endothelial adherens junctions, cell-cell tension, angiogenesis, and barrier formation. *J Cell Biol* 2015;**208**:821–838.
16. van Dijk CG, Nieuweboer FE, Pei JY, Xu YJ, Burgisser P, van Mulligen E, el Azzouzi H, Duncker DJ, Verhaar MC, Cheng C. The complex mural cell: pericyte function in health and disease. *Int J Cardiol* 2015;**190**:75–89.
17. Kofler NM, Cuervo H, Uh MK, Murtomaki A, Kitajewski J. Combined deficiency of Notch1 and Notch3 causes pericyte dysfunction, models CADASIL, and results in arteriovenous malformations. *Sci Rep* 2015;**5**:16449.
18. Winkler EA, Bell RD, Zlokovic BV. Central nervous system pericytes in health and disease. *Nat Neurosci* 2011;**14**:1398–1405.
19. Gaengel K, Genove G, Armulik A, Betsholtz C. Endothelial-mural cell signaling in vascular development and angiogenesis. *Arterioscler Thromb Vasc Biol* 2009;**29**:630–638.
20. Bentley K, Franco CA, Philippides A, Blanco R, Dierkes M, Gebala V, Stanchi F, Jones M, Aspalter IM, Cagna G, Westrom S, Claesson-Welsh L, Vestweber D, Gerhardt H. The role of differential VE-cadherin dynamics in cell rearrangement during angiogenesis. *Nat Cell Biol* 2014;**16**:309–321.
21. Kim SH, Cho YR, Kim HJ, Oh JS, Ahn EK, Ko HJ, Hwang BJ, Lee SJ, Cho Y, Kim YK, Stetler-Stevenson WG, Seo DW. Antagonism of VEGF-A-induced increase in vascular permeability by an integrin alpha3beta1-Shp-1-cAMP/PKA pathway. *Blood* 2012;**120**:4892–4902.
22. Chang F, Lemmon CA, Park D, Romer LH. FAK potentiates Rac1 activation and localization to matrix adhesion sites: a role for betaPIX. *Mol Biol Cell* 2007;**18**:253–264.
23. Paschoud S, Yu D, Pulimeno P, Jond L, Turner JR, Citi S. Cingulin and paracingulin show similar dynamic behaviour, but are recruited independently to junctions. *Mol Membr Biol* 2011;**28**:123–135.
24. Chung PJ, Chi LM, Chen CL, Liang CL, Lin CT, Chang YX, Chen CH, Chang YS. MicroRNA-205 targets tight junction-related proteins during urothelial cellular differentiation. *Mol Cell Proteomics* 2014;**13**:2321–2336.
25. Ohnishi H, Nakahara T, Furuse K, Sasaki H, Tsukita S, Furuse M. JACOP, a novel plaque protein localizing at the apical junctional complex with sequence similarity to cingulin. *J Biol Chem* 2004;**279**:46014–46022.
26. Guo F, Debidda M, Yang L, Williams DA, Zheng Y. Genetic deletion of Rac1 GTPase reveals its critical role in actin stress fiber formation and focal adhesion complex assembly. *J Biol Chem* 2006;**281**:18652–18659.
27. Goetz JG. Bidirectional control of the inner dynamics of focal adhesions promotes cell migration. *Cell Adh Migr* 2009;**3**:185–190.
28. Sussman MA, Welch S, Walker A, Klevitsky R, Hewett TE, Price RL, Schaefer E, Yager K. Altered focal adhesion regulation correlates with cardiomyopathy in mice expressing constitutively active rac1. *J Clin Invest* 2000;**105**:875–886.
29. Choi CK, Chen CS. Jostling for position in angiogenic sprouts: continuous rearrangement of cells explained by differential adhesion dynamics. *embo J* 2014;**33**:1089–1090.